Chinese Journal of Chemical Engineering 28 (2020) 98–103

Contents lists available at ScienceDirect

Chinese Journal of Chemical Engineering

journal homepage: www.elsevier.com/locate/CJChE

Article

Selective swelling of polysulfone/poly(ethylene glycol) block copolymer towards fouling-resistant ultrafiltration membranes☆

Hao Yang, Jiemei Zhou, Zhaogen Wang, Xiansong Shi, Yong Wang *

State Key Laboratory of Materials-Oriented Chemical Engineering, Jiangsu National Synergetic Innovation Center for Advanced Materials, College of Chemical Engineering, Nanjing Tech University, Nanjing 211816, China

ARTICLE INFO

Article history:
Received 19 January 2019
Received in revised form 20 February 2019
Accepted 20 March 2019
Available online 27 March 2019

Keywords:
Polysulfone-*block*-poly(ethylene glycol)
Block copolymer
Fouling resistance
Selective swelling
Ultrafiltration membrane

ABSTRACT

Fouling resistance of ultrafiltration (UF) membranes is critical for their long-term usages in terms of stable performance, so convenient approaches to prepare fouling-resistant membranes are always anticipated. Herein, we demonstrate the facile fabrication of antifouling polysulfone-*block*-poly(ethylene glycol) (PSF-*b*-PEG, SFEG) composite membranes. SFEG layer was coated onto macroporous supports and cavitated by immerging them in acetone/*n*-propanol following the mechanism of selective swelling induced pore generation. Thus-produced SFEG membranes possessed high permeance and excellent mechanical strength. Meanwhile, the structures and separation performances of the SFEG layers can be continuously tuned through simply changing swelling durations. More importantly, the hydrophilic PEG chains were spontaneously enriched onto the pore walls through swelling treatment, endowing intrinsic antifouling property to the SFEG membranes. Bovine serum albumin (BSA)/humic acid (HA) fouling tests proved the prominent fouling resistance of SFEG membranes, and the fouling resistance is expected to be long-standing because of the firm connection between PEG chains and PSF matrix by covalent bonding.

1. Introduction

Polysulfone (PSF) is an extensively used polymer for ultrafiltration (UF) membranes because of the excellent membrane forming ability, thermal stability, chemical durability, and mechanical strength [1–3]. However, the inherent hydrophobic nature of PSF causes strong absorption and accumulation of foulants on the surface and inside pores of membranes during use, resulting in serious membrane fouling [4–6]. Membrane fouling usually leads to severe decline of permeance, reduction of membrane lifetime and additional increase of operation cost [7–9]. Therefore, membrane fouling has been a significant issue that needs to be solved for the industrial applications.

Highly hydrophilic membrane surface is an effective solution to improve fouling resistance of membranes by forming a hydration layer to impede the adsorption between membranes and foulants [10,11].The approaches to improve the surface hydrophilicity of UF membranes mainly include surface adsorption, surface grafting, and surface segregation [7,10]. Compared to surface adsorption/surface grafting that needs a post-modification process and extra manufacturing steps [12,13], surface segregation is an *in situ* modification method. Surface segregation can spontaneously form uniform effective brush layers to acquire access to three-dimensional modification of membranes with amphiphilic materials during the membrane formation process. Therefore, surface segregation is considered as a more convenient technique with the advantages of simple operation and low cost for the hydrophilic modification of membranes [14–16].

Amphiphilic block copolymers (BCPs), which contain both hydrophobic and hydrophilic blocks, are a type of commonly used surface segregation material to modify UF membranes and access antifouling ability for their unique characteristic of microphase separation [17–19]. For example, Hancock *et al.* blended poly(ethylene oxide)/polysulfone (PEO-*b*-PSF) with PSF matrix as precursor to prepare membranes [20]. Upon the phase inversion to generate porous structure, PEO chains tended to migrate to the surface of membrane driven by the hydrophilic nature and their thermodynamical incompatibility with PSF, rendering the high antifouling property of produced membrane. However, BCPs are predominantly utilized as additives by blending with matrix material of membranes, and partial losing during long-term use would lead to the weakening of antifouling performance to some degree.

In recent year, we develop the method to fabricate UF membrane by simply swelling BCPs in selective solvents to the minority blocks, which is called as selective swelling induced pore generation [21–24]. Importantly, the minority polar blocks are gathered around the pore walls

☆ Supported by the National Natural Science Foundation of China (21776126), the National Basic Research Program of China (2015CB655301), the Natural Science Foundation of Jiangsu Province (BK20150063), and partially supported by the Open Fund of State Key Laboratory of Separation Membranes and Membrane Processes (M1-201702).

* Corresponding author.
E-mail address: yongwang@njtech.edu.cn (Y. Wang).

https://doi.org/10.1016/j.cjche.2019.03.011
1004-9541/

during pore formation, leading to the produced membranes with outer surfaces and pore walls uniformly covered by the minority blocks just like surface segregation. The hydrophilicity of minority chains fixed on the membrane surfaces could resist protein adsorption and prevent the decline of permeance. Specifically, we have prepared polystyrene-*b*-poly(ethylene oxide) (PS-*b*-PEO) composite membranes by selective swelling [25]. Antifouling tests showed that PS-*b*-PEO composite membranes exhibited excellent fouling resistance due to the accumulation of PEO chains on membrane surface. This work demonstrates that selective swelling of PEO-containing BCPs provides a novel and convenient method to prepare antifouling UF membranes. However, the polystyrene-based block copolymers generally subject to some practical limits that affect their universal application. On the one hand, the synthetic complexity of PS-based block copolymer causes high production costs. On the other hand, the PS-based membranes usually suffer from poor mechanical integrity as the stiffness and strength of the polystyrene are no match for the commercial PSF membrane. Under the circumstances, the disadvantages of hard synthesis process, high cost and low strength impede the possibility of large-scale approach to produce PS-based membranes.

In the present work, polysulfone-*block*-poly(ethylene glycol) (SFEG), which involves a robust majority block with excellent mechanical strength and a hydrophilic minority block, was employed to design antifouling UF composite membranes. SFEG films as size-selective layer were coated on the PVDF substrates, and whereafter selectively swollen in acetone/*n*-propanol to generate mesopores in the SFEG layer. The produced SFEG membranes possessed high permeance and excellent mechanical strength. Bovine serum albumin (BSA)/humic acid (HA) fouling tests showed the expected fouling resistance of the membranes. On account of the PEG chains being linked to the PSF matrix by covalent bonds, the fouling resistance is expected to be long-standing and will not lessen in service, and this is highly desired for further industrial applications.

2. Experimental

2.1. Materials

The amphiphilic block copolymer PSF-*b*-PEG (SFEG) with the polydispersity index (PDI) of ~2.0, molecular weight (M_w) of 79100 and W (PEG) = 21%, was provided by Nanjing Bangding. All the solvents including 1,2-dichloroethane (>99.0%), acetone (>99.5%), and *n*-propanol (>99.0%) were obtained from Shanghai Lingfeng Chemical Reagent Co., LTD. The macroporous PVDF substrates with 0.22 μm average pore size were purchased from Merck Millipore Ltd. BSA (98%, M_w = 66000) and phosphate buffered solution (PBS) tablets were purchased from MP Biomedicals, LLC. PBS were fabricated through dissolving the PBS tablets in deionized water. HA was purchased from Aladdin. All of the reagents were utilized without further treatment.

2.2. Preparation of SFEG membranes

A desired amount of SFEG was dissolved in 1,2-dichloroethane with a concentration of 0.8 wt%. After mechanical stirring at ambient temperature for over 4 h to insure the complete dissolution of SFEG, the obtained solution was filtrated through a 0.22 μm PTFE filter for three times to remove big aggregates if existed. The SFEG membrane was fabricated *via* coating the SFEG solution onto PVDF substrates. In order to prevent leakage of casting solution, PVDF substrates were soaked in DI water for 20 min to make water fill into the macropores. After removing from water, the water-filled PVDF substrates were placed on a clean glass slide. The SFEG solution was dropped on the PVDF surface and redundant solution was removed by quick swinging prior to complete solvent volatilization. Then, selective swelling process was conducted to generate mesopores in the coated SFEG layer by soaking coated samples into the mixed solvent of acetone/*n*-propanol with the mass ratio of 1/4 at 50 °C for desired durations. Subsequently, the membranes were removed from solvent and dried under ambient conditions.

2.3. Characterizations

The field emission scanning electron microscope (SEM, S-4800, Hitachi) was used to observe the surface and cross-sectional morphologies of SFEG membranes. The membranes were quick-frozen by soaking into liquid nitrogen for 10 s and ruptured to obtain cross-section for SEM characterization. Before SEM characterization, the membrane was sputter-coated with platinum/gold alloy to increase the electrical conductivity. The pore diameter and thickness of the SFEG layer were measured by the Nano-Measure software according to SEM images. The hydrophilicity of the membrane surface was tested *via* a contact angle goniometer (Dropmeter A-100, Maist).

2.4. Filtration tests

The separation performance of SFEG membranes was measured by a dead-end filtration cell (Amicon 8010, Millipore Co.). The filtration tests were operated at room temperature with a 600 $r \cdot min^{-1}$ stirring speed. In the test process, SFEG membrane samples were preloaded with water under 0.1 MPa for 20 min to obtain a stable flux, then the pure water permeance was measured. The 0.5 $g \cdot L^{-1}$ BSA solution dissolving in PBS was used to characterize the rejection properties of the SFEG membranes. The water permeance (J_p) and BSA rejection (R) were obtained *via* Eqs. (1) and (2).

$$J_p = \frac{V}{S \times \Delta t \times p} \tag{1}$$

where J_p ($L \cdot m^{-2} \cdot h^{-1} \cdot MPa^{-1}$), V (L), S (m^2), Δt (h) and p (MPa) are the water permeance, permeated water volume, membrane effective filtration area, operation time, and operation pressure, respectively.

$$R = \left(1 - \frac{C_P}{C_F}\right) \times 100\% \tag{2}$$

where R (%), C_P ($g \cdot L^{-1}$) and C_F ($g \cdot L^{-1}$) are the BSA rejection and concentrations of BSA in the permeation and feed solutions, respectively. C_F is 0.5 $g \cdot L^{-1}$ as preconfigured and C_P is sampled in the permeation solution after filtration tests. The concentrations of BSA solutions were measured by an ultraviolet–visible spectrophotometer (NanoDrop 2000c, Thermo) at the wavelength of 280 nm.

The pressure-resistant property of SFEG membranes was determined *via* testing the pure water fluxes of SFEG membrane under different pressures (0.02–0.4 MPa).

To assess the antifouling property of the SFEG membrane, the membranes were challenged with BSA and HA solutions. The SFEG membrane protein resistance was investigated by BSA static adsorption tests. SFEG membranes were immersed into a container filled with 5 ml of 0.5 $g \cdot L^{-1}$ BSA solution. The container was kept at 25 °C for 24 h to achieve the equilibrium of adsorption/desorption. The BSA adsorption quantity of the SFEG membrane was calculated by different values of BSA solution concentrations before and after adsorption. The HA adsorption ability of membrane was tested in the same way as the measurement of BSA adsorption ability. 10 $mg \cdot L^{-1}$ HA solution was prepared by dissolving a certain amount of HA into 0.1 $mol \cdot L^{-1}$ NaOH solution and then adding deionized water to dilute the solution. 4 $mol \cdot L^{-1}$ HCl solution was used to titrate HA solution to pH 7. Like the BSA adsorption test, the SFEG membranes were immerged into a container filled with 10 ml of 10 $mg \cdot L^{-1}$ HA solution and kept at 25 °C for 24 h. The change of HA solution concentrations before and after adsorption was measured with the UV–vis spectrometer at the wavelength of 229 nm.

The static adsorption quantity of SFEG membranes was calculated by Eq. (3):

$$\mathrm{SAP} = \frac{(C_b - C_a) \times V}{S} \tag{3}$$

where SAP ($\mu g \cdot cm^{-2}$) is the static adsorption quantity of the SFEG membrane and C_b and C_a ($\mu g \cdot ml^{-1}$) are concentrations of BSA or HA solution before and after static adsorption process, respectively. V (ml) and S (cm^2) are the BSA/HA solution volume and membrane effective adsorption area.

The fouling resistance of the SFEG membrane was investigated by testing the flux recovery ratio (FRR). The original pure water permeance of membrane was measured as mentioned above and recorded as J_0 ($L \cdot m^{-2} \cdot h^{-1} \cdot MPa^{-1}$). The membranes were cleaned by water for 10 min after the BSA/HA static adsorption. Afterwards, the pure water permeance was measured again and recorded as J_1 ($L \cdot m^{-2} \cdot h^{-1} \cdot MPa^{-1}$). The FRR (%) was calculated by Eq. (4):

$$\mathrm{FRR} = \frac{J_1}{J_0} \times 100\% \tag{4}$$

3. Results and Discussion

3.1. Morphology of SFEG membrane

Typically, SFEG was coated on PVDF substrate to fabricate the composite membrane. The top surface of the composite membrane with SFEG layer presents a shiny and smooth appearance (Fig. 1a & Video 1) while the bottom surface with PVDF layer maintains originally dull appearance (Fig. 1b & Video 2). SEM characterization shows the as-coated SFEG layer is nonporous with a dense surface (Fig. S1). In order to cavitate the SFEG layer, the composite membranes were soaked into selective solvents, acetone/*n*-propanol, at 50 °C for 60 min and followed by air drying. After swelling, the surface morphology of SFEG membranes was changed from nonporous to nanoporous. According to the surface SEM image of the composite membrane (Fig. 2a), the pores of the SFEG layer are in circular or channel-like shapes and the average pore size is estimated to be approximate 19 nm by overall consulting the widths of channel pores and the diameter of circular pores. The pores are homogeneously distributed on the surface of the SFEG layer. Furthermore, the mesoporous structure spans through the entire SFEG layer and the thickness was 374 nm according to the cross-sectional SEM image (Fig. 2b). The morphology of the SFEG layer is similar to the SFEG membrane spin-coated onto silicon wafer [26]. Compared to SFEG film onto silicon wafer or SFEG self-supporting membrane, the composite membrane can generate mesoporous structure at a low swelling temperature (50 °C) *via* the melioration solvent pair that greatly improves swelling-generation-pore speed and reduces energy consumption. It is noteworthy that the SFEG layer has a strong adhesion with the PVDF substrate as there is no apparent interfacial gap between the two layers (Fig. 2b). From the interface morphology, we could observe that SFEG solution slightly infiltrated into the PVDF macropores. The infiltration would lead to partial filling of SFEG polymer into the PVDF macropores in the top section and further enhanced the attachment between the PVDF substrate and SFEG layer. Moreover, we observed the reverse side of SFEG membrane and discovered this side also kept the original morphology of the macroporous PVDF substrate. This result confirms the SFEG coating solution would not seep to the surface of PVDF substrate. Thus-produced SFEG membranes possess a bilayer composite structure composed of a thin mesoporous SFEG layer on a top macroporous PVDF substrate upside.

The mesoporous structure of the SFEG layer was formed on the strength of the selective-swelling-induced pore generation mechanism [26]. Selective swelling of SFEG to prepare membranes is highly simple without extra addition of modifying materials and no chemical reactions are involved. Before swelling, the PEG microdomains with cylindrical phase were randomly inserted the PSF matrix in the SFEG layer [26–28]. For the following swelling process, acetone/*n*-propanol mixed solvents were chosen as selective solvents. *N*-propanol has a strong affinity to PEG but can barely swell the PSF matrix, while acetone has a moderate affinity to PSF. When the membrane was soaked into the mixed solvents, *n*-propanol was preferentially enriched in the PEG cylinders because of the strong affinity between them. PEG cylinders expanded their volumes and squeezed the PSF phases. When only *n*-propanol was employed, the mobility of PSF chains was poor and the PSF matrix could hardly deform, limiting the generation of pores. Therefore, acetone was introduced to promote the plastic deformation of the PSF matrix. As the swelling proceeded, the expanding PEG cylinders would touch and merge together with nearby PEG cylinders, leading to a consecutive PEG phase distributed in the PSF matrix. After removing the swelling solvents and air-drying, the deformed PSF chains were congealed and their original positions were unrecoverable due to the weakened mobility and the deficiency of impulse with the fast evaporation of both *n*-propanol and acetone. At the same time, the swollen PEG chains collapsed and voids were formed along the positions occupied by PEG cylinders. With pore generation, the collapsed PEG chains were covered on the pore walls and membrane surface.

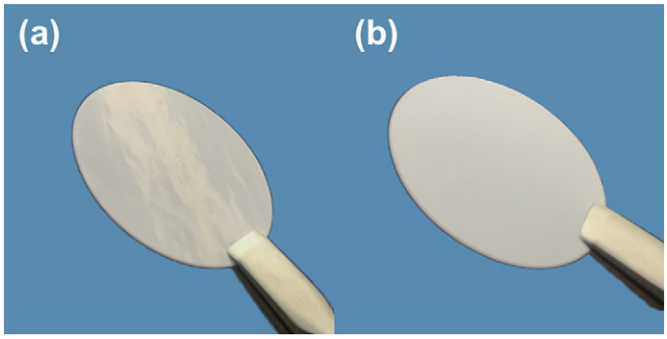

Fig. 1. Photographs of the SFEG membrane: (a) positive side and (b) opposite side.

The morphology of SFEG membranes can be conveniently tailored through changing the swelling durations. Fig. S2 shows the surface morphologies of SFEG layers after swelling in acetone/*n*-propanol at 50 °C for different swelling durations. The morphology and thickness of the SFEG layer of the composite membrane with a PVDF substrate have a similar variation trend compared with the SFEG membrane spin-coated onto silicon wafer [26]. With the prolonging of swelling durations, SFEG layer were swollen to larger degrees, resulting in the increase of pore size and number. When swelling duration is 1 min, some small round pores and few elongated pores appeared on the SFEG layer surface (Fig. S2a). When swelling duration is prolonged to 10 min, the amount and size of pores have increased (Fig. S2b). As the duration reaches to 20 and 30 min, the pores have a continuous increase in diameter and more elongated channel-like pores appeared (Fig. S2c&d). We also observed the cross-sectional morphologies of SFEG membranes with different swelling durations (Fig. S3). The membranes exhibit a dense state across the entire thickness of the SFEG layer with no swelling (Fig. S1b). After swelling treatment, porous morphology is observed and the thickness of the SFEG layer is slightly increased with the prolonging of swelling durations (Fig. 3). The continuously adjustable pore diameter is much desired because it can offer high flexibility and simplification to fabricate membranes with divinable separation performance easily by adjusting the swelling durations.

3.2. Surface hydrophilicity

The surface hydrophilicity of UF membranes plays a critical role in improving permeance and fouling resistance of membranes in UF

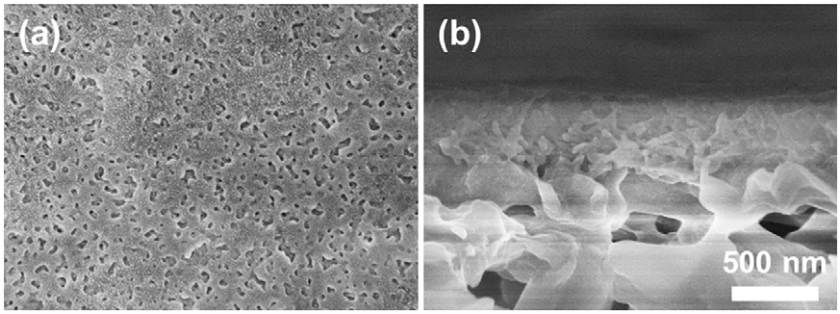

Fig. 2. SEM images of the SFEG membrane swelling in acetone/*n*-propanol at 50 °C for 60 min: (a) the surface morphology, (b) cross-sectional morphology. The images are in the same magnification.

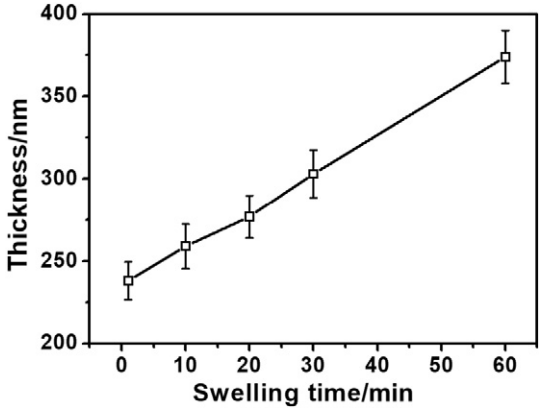

Fig. 3. The thickness of the SFEG layer subjected to acetone/*n*-propanol swelling at 50 °C for different swelling time.

processes. To investigate the effects of swelling durations on surface hydrophilicity of the SFEG membrane, water contact angles (WCAs) of SFEG membranes were measured. As shown in Fig. 4, the SFEG membrane shows a WCA of nearly 90 °C before swelling due to PSF chain enrichment on the membrane surface. More remarkable, after merely swelling at 50 °C for 1 min, the WCA is rapidly reduced to 66° as a result of the surface enrichment of PEG chains. Subsequently, the WCA has a slow decrease to less than 60° with the prolonging of swelling durations. When the swelling duration increased to 60 min, the water contact angle increased a little to more than 60°. According to the Cassie model, the WCA of a porous surface, θ_c, can be estimated using the following equation:

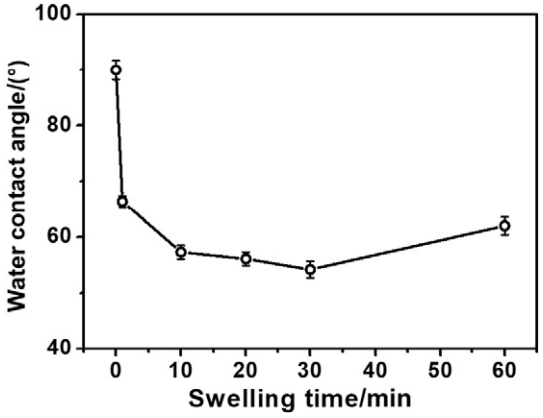

Fig. 4. Water contact angles of the SFEG membranes swelling at 50 °C for different durations.

$$\cos\theta_c = f_s\,(\cos\theta + 1) - 1$$

where f_s is the area fraction of the solid on the surface and θ is the WCA on dense surface. With increasing swelling duration, pores are generally enlarged, leading to decreasing f_s and thus increasing θ_c; meanwhile, more PEG blocks are enriched on the film surface as characterized by XPS, resulting in decreasing values of θ and correspondingly decreasing θ_c. Therefore, the competing effect of decreasing f_s and θ with swelling eventually results in slightly increased WCAs. This change of surface hydrophilicity is consistent with the SFEG membrane coated onto silicon wafer [26]. It is clear that the surface hydrophilicity of the SFEG membrane is enhanced with the swelling treatment owing to the migration of PEG chains onto the membrane surface during the course of swelling as revealed by our previous study [26]. This enrichment of PEG chains occurs along with the generation of pores, and this is much more convenient compared to the PEGylation method of post-modification on membranes [29–31].

3.3. Water permeances and separation performances

We investigated the water permeances and BSA rejection of SFEG membranes fabricated by swelling in different durations. As shown in Fig. 5, the increase of pure water permeance and decrease of BSA rejection can be observed with the prolonging of swelling durations. Before swelling, the membranes displayed no water permeation, implying the dense and defect-free nature of the as-coated SFEG layer. This is coincident with the SEM characterization as discussed above (Fig. S1). In contrast, the SFEG membrane shows a permeance of 104 $L\cdot m^{-2}\cdot h^{-1}\cdot MPa^{-1}$ after swelling for only 1 min, implying the generation of pores throughout the entire membranes. Combined with the morphology observation and WCA change discussed above, it is clear that the SFEG membrane can form mesoporous structure in a very short time (1 min) at relatively low temperature (50 °C), which indicates the high efficiency and much simplicity of the selective swelling method to produce ultrafiltration membranes that would greatly reduce energy consumption. After swelling for 10, 20, 30 and 60 min, the permeances are increased to 2260, 2620, 3210 and 4540 $L\cdot m^{-2}\cdot h^{-1}\cdot MPa^{-1}$, respectively. Meanwhile, the membrane exhibited a 91.7% BSA rejection when swelled for 1 min. For the membranes fabricated with swelling durations of 10, 20, 30 and 60 min, the BSA rejections are reduced to 81.2%, 74.8%, 63.7% and 48.1%, respectively. The increase of permeances is attributed to increased pore sizes and porosities. In addition, we notice that there exists a nonlinear variation relationship between water permeances and swelling durations. This is due to the extended swelling durations caused by the increase of both the pore sizes and SFEG layer thicknesses. The larger pore sizes lead to the increase of water permeances, while the thicker SFEG layer thicknessed tend to decrease the water permeances as a result of increased mass transfer resistance. Meanwhile, the BSA rejections are decreased with the extended swelling durations owing to increased

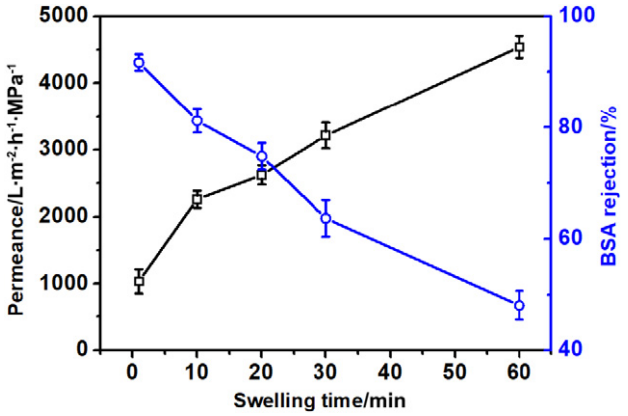

Fig. 5. Pure water permeances and BSA rejections of the SFEG membranes swelling at 50 °C for different durations.

pore sizes. Therefore, both permeances and rejections of the SFEG membranes can be adjusted within a relatively wide range simply *via* adjusting swelling durations, implying the flexibility of selective swelling induced pore generation in preparing tailor-made UF membranes. Furthermore, compared to the self-supporting SFEG membrane reported previously [23], which has a permeance of ~300 $L \cdot m^{-2} \cdot h^{-1} \cdot MPa^{-1}$ and a ~20% BSA rejection, the SFEG membranes possess much higher permselectivity due to the thinner separation layer, improving the performance of membranes greatly. Moreover, swelling durations can tune the swelling degree and change membrane performances, which is one main advantage of the swelling method. In practical use, we can choose the swelling conditions according to the specific requirements for membranes.

3.4. Mechanical stability

The research on the mechanical strength of SFEG membrane swelling at 50 °C for 1 min was carried out using pure water fluxes under different pressures. As shown in Fig. 6, the water flux of the SFEG membrane is linearly correlated with the trans-membrane pressures ranging from of 0.02 to 0.4 MPa. Therefore, the composite membrane with a thin SFEG layer can withstand a pressure as high as 0.4 MPa and has no break as there is no rushed increase in water flux under the pressure up to 0.4 MPa. Even if the SFEG membrane is curved, the SFEG layer would not come off or rupture (Fig. S4). This reasonable mechanical strength of the composite membranes should be ascribed to both the robust PSF skeleton on the SFEG layer and the PVDF supports which provide the mechanical reinforcement.

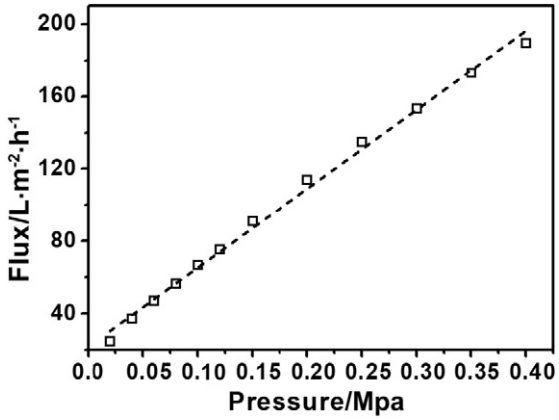

Fig. 6. Pure water flux of the SFEG membranes at various transmembrane pressures.

3.5. Antifouling properties

The fouling resistance of the SFEG membranes was tested by BSA and HA static adsorption experiments. SFEG membranes were soaked in BSA/HA solution for 24 h to reach adsorption equilibrium. As shown in Fig. 7, the swelling-treated SFEG membrane shows lower adsorption amounts of BSA/HA compared to the as-coated SFEG membrane. Meanwhile, the BSA/HA adsorption amounts of the SFEG membranes are gradually decreased with swelling durations. After swelling in acetone/*n*-propanol at 50 °C for 1, 10, 20, 30 and 60 min, the BSA adsorption amounts of membranes are 1104, 764, 510, 340, and 340 $ng \cdot cm^{-2}$, respectively, and the HA adsorption amounts of membranes are 1654, 1459, 1241, 1035, and 672 $ng \cdot cm^{-2}$, respectively. The decrease of BSA/HA adsorption amounts is attributed to the enrichment of PEG chains on the SFEG layer surface and pore wall [26]. PEG is highly hydrophilic and can form hydration shells with water to prevent BSA/HA adsorption.

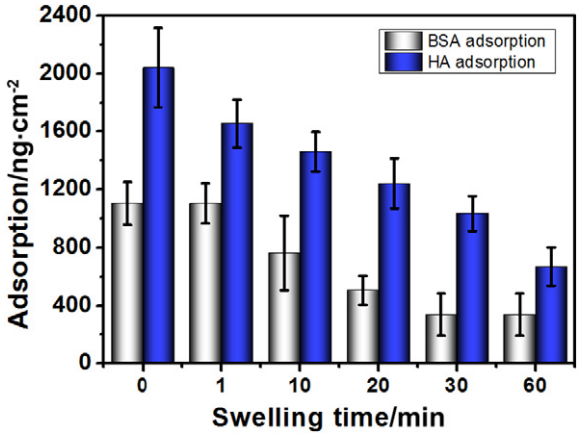

Fig. 7. BSA/HA adsorption of the SFEG membranes fabricated by swelling at 50 °C for different durations.

FRRs were also tested to visualize the antifouling property of the SFEG membranes (Fig. 8). The membranes with different durations were washed with deionized water after BSA/HA adsorption tests and the pure water permeances of the membranes were measured. The FRRs were acquired based on the permeances before and after BSA/HA adsorption. When the foulant was BSA, the FRRs were gradually improved with the increase of swelling durations. With swelling durations for 1, 10, 20, 30 and 60 min, the FRR values of membranes are 85%, 89.4%, 92.1%, 93%, and 95.5%, respectively. Similarly, the FRRs also present an increased tendency with the increase of swelling durations through HA polluting, and the values of FRR are 82.3%, 85.5%, 87%, 87.7%, and 89%, respectively. With the prolonging of swelling durations, more PEG chains migrated to the SFEG membrane surface and the surface hydrophilicity of SFEG membranes is gradually enhanced. The enrichment of PEG and enhanced hydrophilicity improve the fouling resistance, leading to decreased foulant adsorption and increased FRR. Furthermore, the fouling resistance of SFEG membranes is considered to be long-standing as the PEG chains are bonded to the PSF matrix by covalently bonded and would not leak out in the filtration process. This long-standing hydrophilicity and fouling resistance are important advantages of the SFEG membranes fabricated by the selective swelling method.

4. Conclusions

SFEG membranes were fabricated by selective swelling induced pore generation process. The size-adjustable mesoporous SFEG layer serves as the selective layer, and the macroporous PVDF substrate serves as the supporting layer. The SFEG layer possessed interconnected

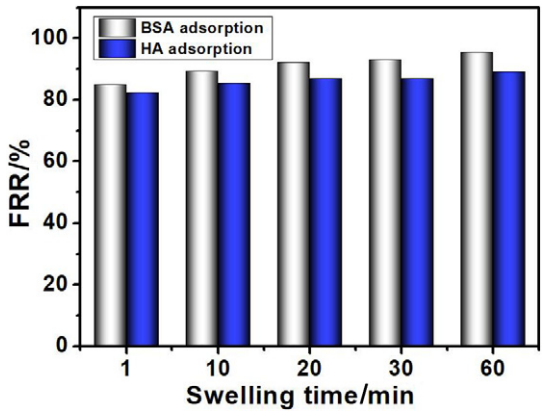

Fig. 8. FRRs of the SFEG membranes fabricated with various swelling durations after BSA/HA adsorption and deionized water washing.

mesopores with tunable sizes by changing the swelling durations. The permeance and filtration performances of SFEG membranes can be tuned within a certain range. Meanwhile, the SFEG membranes possessed good mechanical strength. Importantly, SFEG membranes possessed excellent fouling resistance as proved by low BSA/HA static adsorption and high FRRs because the hydrophilic PEG chains were enriched on the membrane surface. As the SFEG membrane fabricated at 50 °C for 60 min, BSA/HA adsorption amounts were as low as 340/672 ng·cm^{-2} and the flux recovery ratio was up to 95.5%/89%. This work demonstrated a facile strategy to prepare UF membranes with high permeance and excellent fouling resistance.

Acknowledgments

We thank the support from the Program of Excellent Innovation Teams of Jiangsu Higher Education Institutions and the Project of Priority Academic Program Development of Jiangsu Higher Education Institutions (PAPD).

Supplementary Material

Supplementary material to this article can be found online at https://doi.org/10.1016/j.cjche.2019.03.011.

References

[1] Y.N. Yang, H.X. Zhang, P. Wang, Q.Z. Zheng, J. Li, The influence of nano-sized TiO_2 fillers on the morphologies and properties of PSF UF membrane, *J. Membr. Sci.* 288 (2007) 231–238.
[2] K. Zodrow, L. Brunet, S. Mahendra, D. Li, A. Zhang, Q.L. Li, P.J.J. Alvarez, Polysulfone ultrafiltration membranes impregnated with silver nanoparticles show improved biofouling resistance and virus removal, *Water Res.* 43 (2009) 715–723.
[3] J.Y. Park, M.H. Acar, A. Akthakul, W. Kuhlman, A.M. Mayes, Polysulfone-graft-poly (ethylene glycol) graft copolymers for surface modification of polysulfone membranes, *Biomaterials* 27 (2006) 856–865.
[4] A.G. Fane, C.J.D. Fell, A. Suki, The effect of Ph and ionic environment on the ultrafiltration of protein solutions with retentive membranes, *J. Membr. Sci.* 16 (1983) 195–210.
[5] K.J. Kim, A.G. Fane, C.J.D. Fell, D.C. Joy, Fouling mechanisms of membranes during protein ultrafiltration, *J. Membr. Sci.* 68 (1992) 79–91.
[6] J.M. Sheldon, I.M. Reed, C.R. Hawes, The fine-structure of ultrafiltration membranes. 2. Protein fouled membranes, *J. Membr. Sci.* 62 (1991) 87–102.
[7] D. Rana, T. Matsuura, Surface modifications for antifouling membranes, *Chem. Rev.* 110 (2010) 2448–2471.
[8] A. Akthakul, R.F. Salinaro, A.M. Mayes, Antifouling polymer membranes with subnanometer size selectivity, *Macromolecules* 37 (2004) 7663–7668.
[9] M.S. Mauter, Y. Wang, K.C. Okemgbo, C.O. Osuji, E.P. Giannelis, M. Elimelech, Antifouling ultrafiltration membranes via post-fabrication grafting of biocidal nanomaterials, *ACS Appl. Mater. Interfaces* 3 (2011) 2861–2868.
[10] R.N. Zhang, Y.N. Liu, M.R. He, Y.L. Su, X.T. Zhao, M. Elimelech, Z.Y. Jiang, Antifouling membranes for sustainable water purification: Strategies and mechanisms, *Chem. Soc. Rev.* 45 (2016) 5888–5924.
[11] A. Lee, J.W. Elam, S.B. Darling, Membrane materials for water purification: Design, development, and application, *Environ. Sci.: Water Res. Technol.* 2 (2016) 17–42.
[12] X.L. Ma, Y.L. Su, Q. Sun, Y.Q. Wang, Z.Y. Jiang, Enhancing the antifouling property of polyethersulfone ultrafiltration membranes through surface adsorption-crosslinking of poly(vinyl alcohol), *J. Membr. Sci.* 300 (2007) 71–78.
[13] Y. Liu, S.L. Zhang, G.B. Wang, The preparation of antifouling ultrafiltration membrane by surface grafting zwitterionic polymer onto poly(arylene ether sulfone) containing hydroxyl groups membrane, *Desalination* 316 (2013) 127–136.
[14] J.F. Hester, P. Banerjee, A.M. Mayes, Preparation of protein-resistant surfaces on poly (vinylidene fluoride) membranes via surface segregation, *Macromolecules* 32 (1999) 1643–1650.
[15] S. Kang, A. Asatekin, A.M. Mayes, M. Elimelech, Protein antifouling mechanisms of PAN UF membranes incorporating PAN-g-PEO additive, *J. Membr. Sci.* 296 (2007) 42–50.
[16] W.J. Chen, Y.L. Su, J.M. Peng, Y.A. Dong, X.T. Zhao, Z.Y. Jiang, Engineering a robust, versatile amphiphilic membrane surface through forced surface segregation for ultralow flux-decline, *Adv. Funct. Mater.* 21 (2011) 191–198.
[17] W. Zhao, Y.L. Su, C. Li, Q. Shi, X. Ning, Z.Y. Jiang, Fabrication of antifouling polyethersulfone ultrafiltration membranes using Pluronic F127 as both surface modifier and pore-forming agent, *J. Membr. Sci.* 318 (2008) 405–412.
[18] S.F. Wang, J.Y. Feng, Y. Xie, Z.Z. Tian, D.D. Peng, H. Wu, Z.Y. Jiang, Constructing asymmetric membranes via surface segregation for efficient carbon capture, *J. Membr. Sci.* 500 (2016) 25–32.
[19] Y.F. Zhao, P.B. Zhang, J. Sun, C.J. Liu, L.P. Zhu, Y.Y. Xu, Electrolyte-responsive polyethersulfone membranes with zwitterionic polyethersulfone-based copolymers as additive, *J. Membr. Sci.* 510 (2016) 306–313.
[20] L.F. Hancock, S.M. Fagan, M.S. Ziolo, Hydrophilic, semipermeable membranes fabricated with poly(ethylene oxide)–polysulfone block copolymer, *Biomaterials* 21 (2000) 725–733.
[21] Y. Wang, Nondestructive creation of ordered nanopores by selective swelling of block copolymers: Toward homoporous membranes, *Acc. Chem. Res.* 49 (2016) 1401–1408.
[22] N. Yan, Y. Wang, Selective swelling induced pore generation of amphiphilic block copolymers: The role of swelling agents, *J. Polym. Sci. Polym. Phys.* 54 (2016) 926–933.
[23] Z. Wang, X. Yao, Y. Wang, Swelling-induced mesoporous block copolymer membranes with intrinsically active surfaces for size-selective separation, *J. Mater. Chem.* 22 (2012) 20542–20548.
[24] Y. Wang, F. Li, An emerging pore-making strategy: Confined swelling-induced pore generation in block copolymer materials, *Adv. Mater.* 23 (2011) 2134–2148.
[25] H. Yang, Z.G. Wang, Q.Q. Lan, Y. Wang, Antifouling ultrafiltration membranes by selective swelling of polystyrene/poly(ethylene oxide) block copolymers, *J. Membr. Sci.* 542 (2017) 226–232.
[26] Z.G. Wang, R. Liu, H. Yang, Y. Wang, Nanoporous polysulfones with in situ PEGylated surfaces by a simple swelling strategy using paired solvents, *Chem. Commun.* 53 (2017) 9105–9108.
[27] V. Abetz, P.F.W. Simon, Phase behaviour and morphologies of block copolymers, *Adv. Polym. Sci.* 189 (2005) 125–212.
[28] S.B. Darling, Directing the self-assembly of block copolymers, *Prog. Polym. Sci.* 32 (2007) 1152–1204.
[29] X.C. Fan, Y.L. Su, X.T. Zhao, Y.F. Li, R.N. Zhang, T.Y. Ma, Y.N. Liu, Z.Y. Jiang, Manipulating the segregation behavior of polyethylene glycol by hydrogen bonding interaction to endow ultrafiltration membranes with enhanced antifouling performance, *J. Membr. Sci.* 499 (2016) 56–64.
[30] X.Z. Zhao, H.X. Xuan, C.J. He, Enhanced separation and antifouling properties of PVDF ultrafiltration membranes with surface covalent self-assembly of polyethylene glycol, *RSC Adv.* 5 (2015) 81115–81122.
[31] R.M. Gol, S.K. Jewrajka, Facile in situ PEGylation of polyamide thin film composite membranes for improving fouling resistance, *J. Membr. Sci.* 455 (2014) 271–282.